Organic & Biomolecular Chemistry

PAPER

View Article Online
View Journal | View Issue

Cite this: *Org. Biomol. Chem.*, 2019, **17**, 9734

Profiling the oxidative activation of DMSO-F_6 by pulse radiolysis and translational potential for radical C–H trifluoromethylation†

Nico Santschi, * Benson J. Jelier, Samuel Stähelin and Thomas Nauser *

Received 30th September 2019,
Accepted 17th October 2019

DOI: 10.1039/c9ob02119a

rsc.li/obc

The oxidative activation of the perfluorinated analogue of dimethyl sulfoxide, DMSO-F_6, by hydroxyl radicals efficiently produces trifluoromethyl radicals based on pulse radiolysis, laboratory scale experiments, and comparison of rates of reaction for analogous radical systems. In comparison to commercially available precursors, DMSO-F_6 proved to be more stable, easier to handle and overall more convenient than leading F_3C-reagents and may therefore be an ideal surrogate to study F_3C radicals for time-resolved kinetics studies. In addition, we present an improved protocol for the preparation of this largely unexplored reagent.

Introduction

The generation of C-centered radical species R$^{\bullet}$ under laboratory conditions requires suitable precursors, P(R), and a matched set of activating conditions, A, since most of the members of this class of molecules cannot be stored in bottles (Scheme 1). For example, methyl radicals ($H_3C^{\bullet}$) may be accessed most conveniently by the oxidative activation of readily available laboratory solvents, *e.g.* dimethyl sulfoxide (DMSO). For example, the hydroxyl radical (HO$^{\bullet}$) readily generated under traditional Haber–Weiss or Fenton conditions with a suitable Fe(II) additive and hydrogen peroxide liberates the methyl radical from the parent radical precursor. Even though this process is not efficient in terms of yield, its striking operational simplicity allowed studying the important methylation of nucleic acid bases under conditions inspired by Nature.[1] Remarkably, the introduction of a single methyl group into a molecular scaffold can drastically alter a compound's biological profile, typically noted as the magic methyl effect.[2] As a consequence, synthetic organic chemists have dedicated considerable efforts towards expanding and optimizing the arsenal of radical methylation strategies available. For example, Baran and co-workers reported the use of methyl group surrogate radicals ($PhSO_2CH_2^{\bullet}$) accessed by oxidative activation,[3] and Antonchick and co-workers successfully modified the Fenton chemistry approach to achieve introduction of the CD_3 motif on synthetically relevant scales.[4] Similar to the methyl radical, the installation of the trifluoromethyl analogue has garnered significant attention, especially in the past decade. Thus, the sagacious introduction of a single trifluoromethyl group into a organic scaffold typically increases the lipophilicity of a drug candidate (π = 0.88)[5,6] and together with this moiety's chemical inertness, has spurred the design of a host of matched precursor/activator pairs to provide $F_3C^{\bullet}$ radicals (Scheme 1).[7] Two general paradigms exist for the unfettering of the reactive intermediate: (1) reductive activation (RA) of a CF_3-reagent is often employed with photochemical strategies and exploits readily available bulk chemicals such as trifluoroacetic acid derivatives and sulfonyl chlorides[8] whereas (2) oxidative activation (OA) depends on sulfoxide or sulfinate derivatives, *e.g.* Langlois' reagent, which are also inexpensive and readily available. The latter strategy is widely adaptable and by tuning of the sulfinate's substituents, can readily provide access to other alkyl radicals, as most recently demonstrated by Baran and co-workers.[9] Activation of the sulfoxide motif is most often achieved using tBuOOH as stoichiometric reactant and apart from an isolated example by Antonchick and co-workers,[10] we are not aware of a hydroxyl radical being used as a promoter in Fenton-like chemistry. Furthermore, the direct application of the largely unknown, fully fluorinated analogue of the common laboratory solvent, dimethyl sulfoxide, DMSO-F_6 (**1**), as radical precursor to $F_3C^{\bullet}$, *i.e.* in analogy to DMSO serving as precursor to $H_3C^{\bullet}$, is conspicuously absent from the literature. Specifically, in the context of radiolysis experiments, which are carried out in water, the HO$^{\bullet}$ radical constitutes one of the primary products[11] and DMSO-F_6 could potentially provide a convenient entry point into studying the kinetics of $F_3C^{\bullet}$ radicals.

Moreover, DMSO-F_6 would not necessitate specialized handling or additives as required for previously employed gaseous CF_3I or Togni's reagents,[12] nor would we expect any undesired cross-reactivity with commonly employed metal

Eidgenössische Technische Hochschule (ETH) Zürich, Department of Chemistry and Applied Biosciences, Vladimir-Prelog-Weg 1/2, 8093 Zürich, Switzerland.
E-mail: nicosantschi@gmail.com, nauser@inorg.chem.ethz.ch

†Electronic supplementary information (ESI) available. See DOI: 10.1039/c9ob02119a

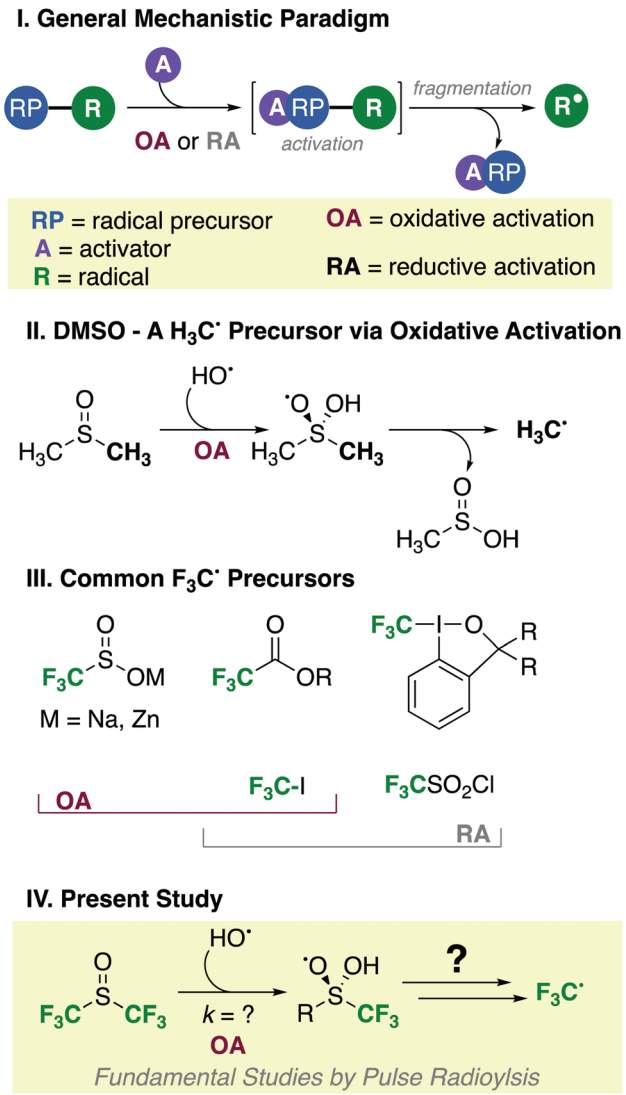

Scheme 1 General mechanistic paradigm for radical production (I), specific case for $H_3C^{\bullet}$ generation (II), common precursors to the trifluoromethyl radical $F_3C^{\bullet}$ and subject of the present study (IV).

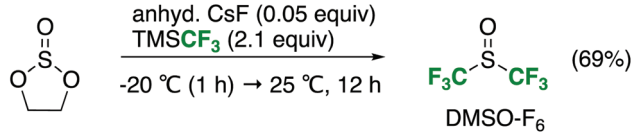

Scheme 2 Improved synthesis of DMSO-F_6.

salts. Furthermore, the abovementioned commercial zinc sulfinate radical precursors are of limited use due to the formation of a precipitate with $K_4[Fe^{II}(CN)_6]$,[13] one of the standard indicators for $HO^{\bullet}$ radicals. Herein, we explored the chemical kinetics of DMSO-F_6 with primary radiolysis products, juxtapose these values with parameters available for DMSO in the literature, and perform preliminary activation test of DMSO-F_6 with Fenton's reagent as a foundational study for an alternative radical trifluoromethylation reagent.

Materials and methods

Synthesis of DMSO-F_6

The synthesis of perfluorodimethylsulfoxide, DMSO-F_6, is based on a sole literature report from 1972.[14,15] However, the reported procedure (A) (requiring heating substantially above the boiling point of the product, and a substantial but delayed exotherm) required significant improvements to negate an unsafe and questionable protocol, to remove ambiguity, and update key spectroscopic details of DMSO-F_6. Spectroscopic examination only available by extended ^{13}C NMR experiments revealed that product A was only about 70% estimated purity (measured against an internal standard by ^{19}F NMR with a pulse delay value, d_1, of 10 s) using the reported procedure as the by-products including TMS-F and Me_3SiOMe form an inseparable ternary azeotropic mixture. We were not able to purify the mixture properly by any number of fractional distillations or liquid–liquid extraction. Therefore, an alternative synthesis strategy (B) was developed which led to the desired product with a purity of >95% based on GC-MS analysis (Scheme 2).

Thus, a 350 mL oven-dried Ace Glass pressure vessel was charged with CsF (0.978 g, 6.44 mmol, 0.05 equiv.) and a large pTFE stirbar and subsequently dried at 200 °C at 1×10^{-2} mbar for 12 h and then backfilled with dry argon. The reaction vessel was cooled to RT and then to −20 °C in an EtOH bath by means of externally controlled circulator. 1,3,2-Dioxathiolane 2-oxide (14.09 g, 130 mmol, 1.0 equiv.) and $TMSCF_3$ (38.20 g, 269 mmol, 2.1 equiv.) were added under an argon atmosphere. The flask was sealed and the contents were stirred at −20 °C for 1 h, warmed to RT and stirred for an additional 22 h behind a blast shield. To prevent loss of the volatile DMSO-F_6 during post-reaction workup, the light-yellow crude reaction mixture was cooled to 0 °C, and the contents transferred to a distillation apparatus containing a 25 cm rectifying column. The product was fractionally distilled twice, collecting the fraction with a b.p. of approx. 34 °C at 760 mmHg to afford hexafluorodimethylsulfoxide (DMSO-F_6) as a colourless, volatile liquid (16.63 g, 69% yield) still containing trace trimethylsilyl impurities (*ca.* <5% by GC-MS). **^{1}H NMR** = *product contains no protons*. **^{13}C NMR** (101 MHz, $CDCl_3$) δ 123.59 ppm (qm, $^1J_{CF}$ = 338 Hz). Residual TMSF is observed at −0.1 ppm (d, $^2J_{CF}$ = 15.3 Hz). **^{19}F{^{1}H} NMR** (282.38 MHz, $CDCl_3$, 298 K, int. ref. to 2.5% w/w $CFCl_3$) −67.45 ppm (s, 6F) (previously reported at 64.5 ppm (ref. 14)). **IR** (ATR-diamond, cm^{-1}): 942, 955, 1100, 1119, 1182, 1244. GC-MS (EI, 70 eV) and IR were also previously reported by Shreeve and are consistent with our observations (see ESI† for complete analysis).[14]

Most experiments with DMSO-F_6 were carried out with product derived from Method A. If the contaminants were less reactive than DMSO-F_6, then kinetics results are expected to be essentially unaffected. Alternatively, if the trimethylsilyl fluoride contaminants were significantly more reactive than DMSO-F_6, then the derived reaction rates will be too high.

Controls (section 3) with product from Method B (see below) yielded comparable kinetics results as observed with product A. In keeping with expectations, rates derived with product A are smaller than rates derived with product B.

Vapor pressure of DMSO-F_6

The unbuffered sample solutions were thoroughly degassed and then saturated with a specific gas or gas mixture before addition of DMSO-F_6. To this end, 50 μL of the reagent (product A or B) were added to the closed vessel containing 10 mL of sample solution (ρ = 1.42 g cm^{-3} (see ESI†)), thereby minimizing losses by evaporation. The solution was then taken up with a Sample-Lock Syringe (Hamilton) and introduced into the irradiation cell by a syringe pump through PEEK tubing. DMSO-F_6 is highly volatile. We assumed that we observe the vapor pressure over a binary mixture of liquids, *i.e.* DMSO-F_6 in water. In this case, the amount of DMSO-F_6 in solution is dependent on its vapor pressure and the volume of the gas-phase. The assumption was validated and the vapor pressure derived as follows:

(A) The concentration of DMSO-F_6 remaining in the solution is proportional to its scavenging power. This was derived by appropriate competition experiments (section 3) with solutions prepared in a Schlenk tube with known volume. Three experiments were carried out with an identical solution. For each experiment, 10 ml solution were put in the same Schlenk tube and saturated with N_2O. Then, 0 μL, 50 μL or 100 μL DMSO-F_6 were added. Therefore, 0 mM DMSO-F_6, x mM DMSO-F_6, and (x + 38) mM DMSO-F_6, respectively, are present in the solutions. The (38 – x) mM DMSO-F_6 end up in the gas-phase. With the known volume of the Schlenk tube we estimated a vapor pressure of approx. 250 mbar at 22 °C.

(B) A 10 ml solution of 3 mM Ferrocyanide ($K_4[Fe(CN)_6]$), saturated with N_2O, was spiked in a gas-tight sample-lock syringe (Hamilton) with 50 μl DMSO-F_6. This corresponds to a concentration of 38 mM, and the derived rate constants k_4 and k_7 agree with the rate constants derived above (see section 3).

(C) 10 ml water at 24 °C was saturated in a Schlenk tube with N_2O to a total gas-pressure of 930 mbar. Then subsequently two portions of 50 μl DMSO-F_6 each were added. The total pressures in the Schlenk-tube measured after the additions were 1230 mbar and 1234 mbar, again in agreement with our assumption of a liquid–vapor equilibrium.

Methods

Radicals were generated by pulse-irradiation of unbuffered aqueous solutions with ionizing radiation (2 MeV-electrons) and the products of this pulsed radiolysis are known (eqn (1)).[11]

$$H_2O \xrightarrow{h\nu} HO^\bullet + H^\bullet + e^{\bullet-} + H_2 + H_2O_2 + H^+ \quad (1)$$

The applied radiation deposits energy mass-proportionally and therefore, in dilute solution, all energy is transferred to the solvent. The product distribution and the yield of water radiolysis are known and depend on the applied dose. Specifically, the yields ("G-values") are $G(e_{aq}^-)$ = 2.65, $G(HO^\bullet)$ = 2.65, $G(H^+)$ = 2.65 and $G(H^\bullet)$ = 0.55 with G-values given in species per 100 eV deposited dose. If the sample solution is saturated with N_2O prior to radiolysis (at 298.15 K: $\chi_1 = 4.367 \times 10^{-4}$, $[N_2O]_{sat}$ = 24.2 mM),[16] then the solvated electrons e_{aq}^- can also be converted to $HO^\bullet$ according to eqn (2), thereby doubling the yield of this oxidizing species.

$$N_2O + e_{aq}^{\bullet-} + H^+ \rightarrow HO^\bullet + N_2 \quad (2)$$

Note, that if other fast reactions with $e_{aq}^{\bullet-}$ do occur, they may compete with reaction (2). In particular and in analogy with other halogenated substances and carbonyl-derivatives, DMSO-F_6 is also expected to react quickly with $e_{aq}^{\bullet-}$. As a consequence, for our kinetics analyses we aim for a ratio

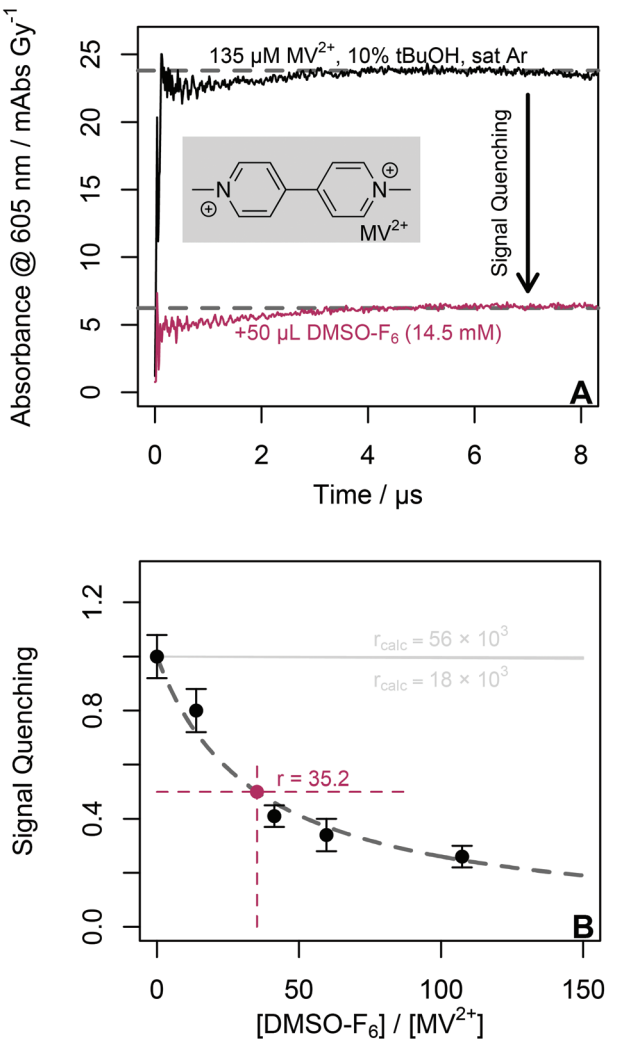

Fig. 1 (A) Temporal evolution of dose-normalized absorbance at 605 nm after irradiation (10 Gy) of an argon saturated solution of methyl viologen MV^{2+} (135 μM) and tBuOH (10%, 1.1 mM) in absence (black) and presence (maroon) of DMSO-F_6 (14.5 mM). (B) The ratio $[MV^{\bullet+}]/[MV^{\bullet+}]_0$ varies non-linearly with the ratio $[DMSO\text{-}F_6]/[MV^{2+}]$. At $[DMSO\text{-}F_6]/[MV^{2+}]$ = 35.2, half the solvated electrons e_{aq}^- are intercepted by DMSO-F_6. In light grey, predicted ratios $[MV^{\bullet+}]/[MV^{\bullet+}]_0$ for DMSO based on kinetic data available in the literature. Error bars represent two standard deviations.

$(k(N_2O + e_{aq}^{\bullet-}) \times [N_2O]_{sat})/(k(\text{DMSO-F}_6 + e_{aq}^{\bullet-}) \times [\text{DMSO-F}_6]) \geq 10$, which correspond to >90% of the $e_{aq}^{\bullet-}$ being scavenged by N_2O.

In certain experiments tBuOH was used as a HO$^{\bullet}$–scavenger to avoid interferences by this oxidizing species (eqn (3)).

$$(CH_3)_3COH + HO^{\bullet} \rightarrow (CH_3)_2C(OH)CH_2^{\bullet} + H_2O \quad (3)$$

The rate constant of the reaction of a $CF_3^{\bullet}$-precursor with a radical was always determined by competition with an indicator reaction. As example see reaction (4) and competitor in reaction (5). The product yield is given by eqn (6a) and results are shown in Fig. 1B. The data were not linearized for analysis, because such treatment would amplify the influence of measurement errors. Instead, a least squares fit according to eqn (6b) was performed by variation of the parameter r. Thus, errors were dominated by the uncertainties in the rate constants used as references.

Results

Reaction of DMSO-F$_6$ with $e_{aq}^{\bullet-}$

The rate constant k_4 was determined by competition with methyl viologen (MV^{2+}), reaction (5), observing the intensely blue colored methyl viologen radical ($MV^{\bullet+}$) at 605 nm ($\varepsilon_{605} = 1.31 \times 10^4$ M^{-1} cm^{-1}).[17]

$$\text{DMSO-F}_6 + e_{aq}^{\bullet-} \rightarrow \text{products} \quad (4)$$

$$MV^{2+} + e_{aq}^{\bullet-} \rightarrow MV^{\bullet+} \quad (5)$$

Addition of DMSO-F$_6$ to a solution of MV^{2+} suppresses the formation of $MV^{\bullet+}$ (Fig. 1) and competition predicts

$$[MV^{\bullet+}] = [MV^{\bullet+}]_0 \times (k_5[MV^{2+}])/(k_5[MV^{2+}] + k_4[\text{DMSO-F}_6]) \quad (6a)$$

$$[MV^{\bullet+}]/[MV^{\bullet+}]_0 = (r[MV^{2+}])/(r[MV^{2+}] + [\text{DMSO-F}_6]) \quad (6b)$$

$$r = k_5/k_4 \quad (6c)$$

with $[MV^{\bullet+}]_0$ the yield in absence of DMSO-F$_6$. The product concentration was measured as temporal average over 4–6 μs after the pulse. When 14.5 mM DMSO-F$_6$ was introduced to an argon saturated solution containing 135 μM MV^{2+} and 10% tBuOH, the absorbance at 605 nm was lowered by 74% from 23.8 to 6.3 mAbs Gy^{-1} (Fig. 1A). Variation of $[MV^{2+}]$ (0.135, 0.24, 0.35, 1.05 mM) at constant [DMSO-F$_6$] leads to Fig. 1B and to $k_5/k_4 = 35.2$ with a least squares fit of eqn (6b). With $k_5 = (5.4 - 9.0) \times 10^{10}$ M^{-1} s^{-1},[18] we derive $k_4 = (1.5 - 2.6) \times 10^9$ M^{-1} s^{-1}.

Based on the rate constant $k_2 = (8.0 - 9.6) \times 10^9$ M^{-1} s^{-1} and the solubility of N_2O in water at 298.15 K, $[N_2O]_{sat} = 24.2$ mM, we calculate that 84–91% of the solvated electrons are scavenged by N_2O in presence of 14.5 mM DMSO-F$_6$,[19a,20] in close agreement to our aim. In consequence, G(HO$^{\bullet}$) = 4.87–5.07 and G(reaction (4)) = 0.23–0.43. Note, however, that this does not affect our competition experiments because the branching ratio for electrons through reactions (2) and (4) was always constant if DMSO-F$_6$ was used.

Reaction of DMSO-F$_6$ with HO$^{\bullet}$

The rate constant k_7 was determined by competition with hexacyanoferrate(4-) ("ferrocyanide") and hexachloroiridate(3-) (Fig. 2, maroon and green, respectively). Each data point is an average of >4 single determinations:

$$\text{DMSO-F}_6 + HO^{\bullet} \rightarrow [(CF_3)_2S(OH)O]^{\bullet} \quad (7)$$

$$Fe^{II}(CN)_6^{4-} + HO^{\bullet} \rightarrow Fe^{III}(CN)_6^{3-} + HO^{-} \quad (8)$$

$$Ir^{III}Cl_6^{3-} + HO^{\bullet} \rightarrow Ir^{IV}Cl_6^{2-} + HO^{-} \quad (9)$$

DMSO-F$_6$ (14.5 mM) was added to aqueous, unbuffered and N_2O saturated solutions of $Fe^{II}(CN)_6^{4-}$ (0.11–1 mM). After pulse irradiation with doses of 10–20 Gy yields were compared to respective measurements with 0.11 mM $Fe^{II}(CN)_6^{4-}$ in the absence of DMSO-F$_6$. The reaction was followed spectroscopically at 420 nm ($\varepsilon_{420}(Fe^{III}(CN)_6^{3-}) = (0.9 - 1.1) \times 10^3$ M^{-1} cm^{-1}) and the final absorption ("yield") was determined as a temporal average over 4–8 μs after the pulse.[21] Alternatively, 14.5 mM DMSO-F$_6$ was added to aqueous, unbuffered, N_2O saturated solutions of 97, 291 and 873 μM $Ir^{III}Cl_6^{3-}$. Solutions were pulse-irradiated, the kinetics was followed at 435 nm and plotted with reference to a solution of 97 μM $Ir^{III}Cl_6^{3-}$ in the absence of reagent. Both, reaction (8) and (9), are diffusion controlled with $k_8 = (0.92 - 1.1) \times 10^{10}$ M^{-1},[22] and $k_9 = (0.47–1.3) \times 10^{10}$ M^{-1}.[23] Given $k_8/k_7 = 4.8$ and $k_9/k_7 = 6.4$ (Table 1), we derive $k_7 = (0.73–2.5) \times 10^9$ M^{-1} s^{-1}. The uncertainty in k_7 originates from the large uncertainty in k_9 (see Table 1) and, therefore, the upper limit of the given range has the higher probability of being correct.

At longer timescales we observe in both cases additional processes, which we cannot explain quantitatively (see ESI†). The processes are clearly dose-dependent, suggestive for invol-

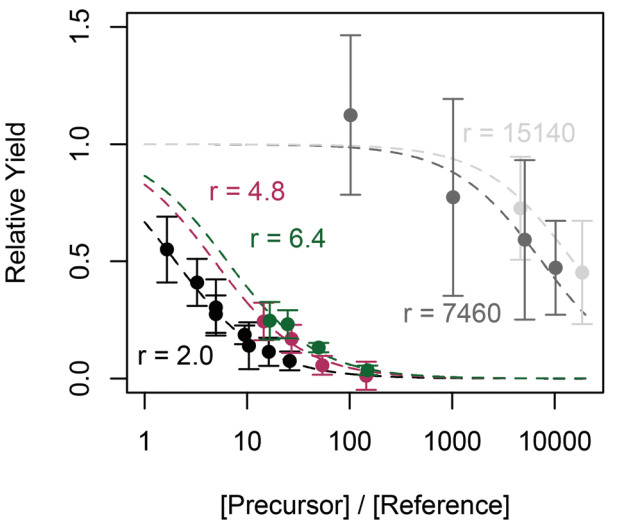

Fig. 2 Relative yield of reference oxidation reaction for different [Precursor]/[Reference] ratios. Precursors to $F_3C^{\bullet}$ employed as competitors: DMSO-F$_6$ (magenta, green), Langlois' reagent (black) and trifluoroacetate (light and dim grey). Error bars represent two standard deviations.

Table 1 Compilation of literature reference rates, k(Ref. + HO$^\bullet$), and thereof derived rate constants for oxidative activation of $F_3C^\bullet$ precursors, k(P + HO$^\bullet$)

Precursor (P)	Reference (Ref.)	k(Ref. + HO$^\bullet$)/ 10^{10} M^{-1} s^{-1}	k(Ref. + HO$^\bullet$)/ k(P + HO$^\bullet$)	k(P + HO$^\bullet$)/ M^{-1} s^{-1}
DMSO-F_6	$Fe^{II}(CN)_6^{4-}$	0.92–1.1 (ref. 22)	4.8	$(1.9–2.5) \times 10^9$
	$Ir^{III}Cl_6^{3-}$	0.47–1.3 (ref. 23)	6.4	$(0.73–2.0) \times 10^9$
$F_3CSO_2^-$	$Fe^{II}(CN)_6^{4-}$	0.92–1.1 (ref. 22)	2.0	$(4.6–5.5) \times 10^9$
$F_3CCO_2^-$	$Fe^{II}(CN)_6^{4-}$	0.92–1.1 (ref. 22)	15 140	$(6.1–7.3) \times 10^5$
	SCN^-	1.4 (ref. 24)	7460	1.8×10^6

vement of recombination reactions, *i.e.* reactions of/with products. Reaction (7) will be followed most probably by a fragmentation and we assume that $CF_3S(O)O^-$ and $F_3C^\bullet$ are formed (see below, reaction (14)). The sulfinate is a reducing agent and $F_3C^\bullet$ is a moderately potent oxidant. It is not surprising that such species would further react in a mixture with the partially oxidized competitors and, therefore, induce concentration change of oxidized indicator.

Controls with product B

Competition according to section 1 was reproduced and r = 17.9 was derived, *i.e.* $k_4 = (3 - 5) \times 10^9$ M^{-1} s^{-1}. For the determination of the vapor pressure and the concentration of DMSO-F_6 in a given Schlenk-tube, we measured the yield of $Fe^{III}(CN)_6^{3-}$ (see above). Experiments were carried out with 0, 50 μl and 100 μl DMSO-F_6. With N_2O saturated solution of 3 mM $Fe^{II}(CN)_6^{4-}$ we derived k_4 using the branching of solvated electrons *via* reactions (2) and (4). We observe a two stage reaction, a fast initial reaction followed by a slower process of pseudo-first order with $k_{obs} = 2 \times 10^4$ s^{-1}. Under the assumption that the total yield $G(Fe^{III}(CN)_6^{3-})_{tot} = G(OH^\bullet)$ and that $G(OH^\bullet) + G(e_{aq}^{\bullet-}) = 5.8$[25] we estimate $k_4 = (3.4 - 4.1) \times 10^9$ M^{-1} s^{-1}. This assumption implies also, that the initial, fast absorption increase is due to reaction (8) and the slower is a consequence of reaction (7). Therefore, $G(Fe^{III}(CN)_6^{3-})_{initial}/G(Fe^{III}(CN)_6^{3-})_{tot} = k_8[Fe^{II}(CN)_6^{4-}]/(k_8[Fe^{II}(CN)_6^{4-}] + k_7[DMSO\text{-}F_6])$. We derive a rate constant of $k_7 = (0.83 - 1.0) \times 10^9$ M^{-1} s^{-1}. If 10 ml of a N_2O saturated solution of 3 mM $Fe^{II}(CN)_6^{4-}$ was directly spiked in the sample-lock syringe with 50 μl DMSO-F_6, we derive $k_4 = (1.7 - 4.7) \times 10^9$ M^{-1} s^{-1} and $k_7 = (0.63 - 2.0) \times 10^9$ M^{-1} s^{-1}.

Reaction of $CF_3SO_2^-$ (Langlois' reagent) with HO$^\bullet$

The reaction rate was measured in competition with reaction (8):

$$CF_3SO_2^- + HO^\bullet \rightarrow [CF_3SO_2OH]^{\bullet-} \quad (10)$$

Unbuffered, N_2O saturated, aqueous solutions of 10.4 mM CF_3SO_2Na and varying concentration of $K_4Fe^{II}(CN)_6$ were pulse-irradiated with doses of 10–20 Gy. Two independent experimental series were measured, (1) $[K_4Fe^{II}(CN)_6]$ = 0.4–6.3 mM and (2) $[K_4Fe^{II}(CN)_6]$ = 0.63–3 mM. As reference a solution of 1.1 mM $K_4Fe^{II}(CN)_6$ was used. Results are shown in Fig. 2 (black) and for the obtained value of r = 2 we arrive at $k_{10} = (4.6–5.5) \times 10^9$ M^{-1} s^{-1} (Table 1).

Also with Langlois' reagent we observed reactions at later times, however, the reproducibility of those measurements was unsatisfactory. We suspect a non-negligible influence of impurities on our measurements at times >20 μs after pulse. While the corresponding Zn-salt is also commercially available and is typically provided in much better quality, its use is prohibited by the formation of Zn^{2+} precipitates with ferrocyanide (*vide infra*).[13]

Reaction of $CF_3CO_2^-$ with HO$^\bullet$

The rate constant of this reaction was measured *versus* ferrocyanide and thiocyanate:

$$CF_3CO_2^- + HO^\bullet \rightarrow F_3C^\bullet + CO_2 + HO^- \quad (11)$$

$$SCN^- + HO^\bullet \rightarrow SCN^\bullet + HO^- \quad (12)$$

$$SCN^- + SCN^\bullet \rightarrow (SCN)_2^{\bullet-} \quad (13)$$

The ratio k_8/k_{11} = 15 140 was determined in unbuffered, N_2O saturated aqueous solutions containing either 0.11 mM $K_4Fe^{II}(CN)_6$/0.5 M $CF_3CO_2^-$ or 0.05 mM $K_4Fe^{II}(CN)_6$/1 M $CF_3CO_2^-$ (Fig. 2, light grey). As reference, a solution of 0.11 mM $K_4Fe^{II}(CN)_6$ was chosen.

Thiocyanate is often used as dosimeter in pulse radiolysis, reaction (13) is an equilibrium reaction, and $(SCN)_2^{\bullet-}$ has a known molar absorptivity of $\varepsilon_{475}((SCN)_2^{\bullet-}) = 7580$ M^{-1} cm^{-1}.[26] Unbuffered, N_2O saturated solutions of 510 mM $CF_3CO_2^-$ and 0.05–5 mM KSCN were pulse-irradiated and k_{12}/k_{11} = 7460 determined. It is noteworthy that (pseudo-)halogenide radicals tend to form complexes with anions, *e.g.* reaction (13), and for chlorine atoms even the diffusion-controlled reaction with hydroxide is described.[27] Possibly, $SCN^\bullet$ will react with the 0.5 M carboxylate present and such an equilibrium would compete with equilibrium (13) resulting, in turn, in an overestimation of k_{11}.

2,2′-Azino-bis(3-ethylbenzothiazoline-6-sulphonic acid ($ABTS^{2-}$) as indicator for the reaction mechanism

One-electron oxidation of $ABTS^{2-}$ produces a strongly colored radical, $ABTS^{\bullet-}$, with $\varepsilon_{414} = 3.6 \times 10^4$ M^{-1} cm^{-1}.[28] It is a convenient reagent to test for a moderately or strongly one-electron oxidizing species in a solution. We suspect $[(CF_3)_2S(HO)O]^\bullet$ (reaction (7)) to be of low reactivity and wished to gain kinetics information on reaction (14). Reaction (16) is very fast, $k_{16} = (1.2–1.9) \times 10^9$ M^{-1} s^{-1}, and we suspect k_{17} to be of similar magnitude, large enough to possibly monitor reactions (14) and/or (15).

$$[(CF_3)_2S(OH)O]^\bullet \rightarrow CF_3SO_2^- + F_3C^\bullet + H^+ \quad (14)$$

$$F_3C^\bullet + O_2 \rightarrow F_3COO^\bullet \quad (15)$$

$$ABTS^{2-} + Cl_3COO^\bullet \rightarrow ABTS^{\bullet-} + Cl_3COOH + HO^- \quad (16)$$

$$ABTS^{2-} + F_3COO^\bullet \rightarrow ABTS^{\bullet-} + F_3COOH + HO^- \quad (17)$$

$$ABTS^{2-} + HO^{\bullet} \rightarrow ABTS^{\bullet -} + HO^{-} \quad (18)$$

$$H^{\bullet}/e_{aq}{}^{\bullet -} + O_2 \rightarrow O_2{}^{\bullet -}/HO_2{}^{\bullet} \quad (19)$$

Solutions were saturated with a gas mixture of $N_2O : O_2 \approx 5 : 1$. This will change the yields of the different radicals compared to experiments with N_2O saturation, as we have an additional reaction (19). If gas-saturation were perfectly reproducible, no variation of starting conditions after the pulse is expected. We measured DMSO-F_6 (14.5 mM) in presence of $ABTS^{2-}$ (59, 98, 137 μM) and, as a reference in absence of DMSO-F_6, we used 98 μM $ABTS^{2-}$ (Fig. 3, black). For this latter case, we determined $k_{18} = 1.3 \times 10^{10}$ M^{-1} s^{-1}, in agreement with the reported value.[28] The initial absorption of the kinetics traces, directly after the pulse, increases with increasing $[ABTS^{2-}]$, consistent with the aforementioned rate constant k_{18}. Also, we observe that the yield of $[ABTS^{\bullet -}]$ in reaction (18) is only about 57%, in full agreement with the work of Willson.[28]

The gas was mixed manually for every stock solution. We observed slightly increased yields of $ABTS^{\bullet -}$ with each new solution. The effect was not dependent on the $ABTS^{2-}$ concentration, as the different concentrations were measured in random order. The total signal increase over the whole day was approximately 15% (see ESI†). We judged that we were observing an artifact and, therefore, normalized the curves for the same end-absorption.‡ Normalization does not influence the derived rate constants. Kinetics traces can be seen in Fig. 3. The kinetics change dramatically in the presence of DMSO-F_6, and there are three important qualitative observations: (i) the reactions are distinctly slower, (ii) instead of a 1st order growth we observe a lag-phase followed by an absorption increase to the level observed before and (iii) the rate of increase is dependent on $[ABTS^{2-}]$. The lag-phase (ii) is typical for multi-step reactions, in support of our assumptions. We infer to observe consecutive reactions of reaction (7), presumably reactions (14), (15) and (17). It even seems, that the total yield of $ABTS^{\bullet -}$ is independent whether $ABTS^{2-}$ is oxidized directly *via* reaction (18) or indirectly *via* a reaction cascade starting at reaction (7).

Based on these qualitative observations we set out to model the kinetics traces. Again, we suspect a reaction cascade involving reactions (7), (14), (15) and (17). For our simulation of the shape of the curve, reaction (7) is irrelevant for the kinetics because it has a half-life of only $t_{\frac{1}{2}} = \ln(2)/(k_7 \times [\text{DMSO-F}_6]) < 80$ ns (for $k_7 > 0.6 \times 10^9$ M^{-1} s^{-1}). We know that reaction (17) is relevant, because the rate of absorption build up in Fig. 3 (color) is clearly dependent on $[ABTS^{2-}]$.

Because we want to limit the number of parameters in our model, we tried to model reactions (14) and (15) together using one single first order rate constant k_{calc}. With $[O_2] \gg [F_3C^{\bullet}]$, this would imply that either $k_{calc} = k_{14} \gg k_{15}[O_2]$ or $k_{calc} = k_{15}[O_2] \gg k_{14}$. In the case that $k_{calc} = k_{15}[O_2]$, the process of gas saturation would govern the results. The oxygen concentration, $[O_2]$, in the samples were not analytically quantified between samples of DMSO-F_6 and therefore different oxygen concentrations could additionally provide a rationale for slightly different values observed between experimental series (Table 2). It is foreseeable that measured values for reactions (14) and (17) will also be subject to the analytical quality of DMSO-F_6 used.

The corresponding least-square fitted curves can be seen in Fig. 3, the corresponding parameters are shown in Table 2.

‡ In the controls, this effect was not observed anymore.

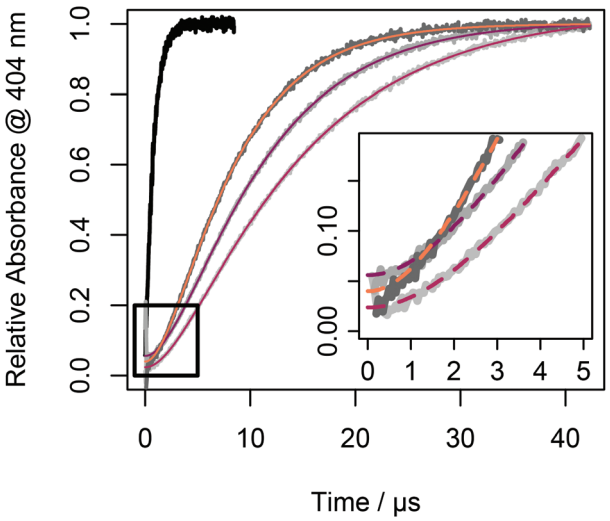

Fig. 3 Normalized temporal evolution of absorbance at 404 nm for $ABTS^{2-}$ solutions saturated in $N_2O : O_2 = 5 : 1$ after irradiation with 10 Gy. Addition of $DMSOF_6$ (14.5 mM) to the $ABTS^{2-}$ solution (98 μM) leads to a change in overall kinetics from *pseudo*-first order (black) to consecutive reactions (salmon). Rate of oxidation depends on the initial $ABTS^{2-}$ concentration and increases in the order 59 μM (maroon), 98 μM (salmon) and 137 μM (purple). Inset: magnified area as encompassed by black rectangle to highlight initial offset and sigmoidal curve shape. Colored line segments are model fits.

Table 2 Compilation of model parameters for modeling the system comprising of eqn (14), (15) and (17)

$[ABTS^{2-}]$/μM	$k_{calc}{}^{a}/10^5$ s^{-1}	$k_{17}{}^{b}/10^9$ M^{-1} s^{-1}	Offset/10^{-3} Gy
59[c]	2.7 ± 0.7[b]	1.5 ± 0.3[b]	2.4
98[c]	2.7 ± 0.2[b]	1.2 ± 0.0[b]	5.6
137[c]	3.6 ± 0.4[b]	1.2 ± 0.1[b]	4.0
68[d]	0.6 ± 0.02[b]	2.9 ± 0.1[b]	2.7
125[d]	0.9 ± 0.08[b]	2.3 ± 0.2[b]	4.5
250[d]	1.1 ± 0.02[b]	2.6 ± 0.1[b]	10

[a] First order intermediate step. [b] Standard deviations based on fitting $N \geq 5$ kinetics traces. [c] Experiments performed with product A. [d] Experiments performed with product B.

Fenton reaction in presence of DMSO-F_6 and product analysis

We characterized the radical species generated by oxidative activation by its reaction with caffeine. This xanthine is an ideal substrate: it is water soluble, features only one reactive

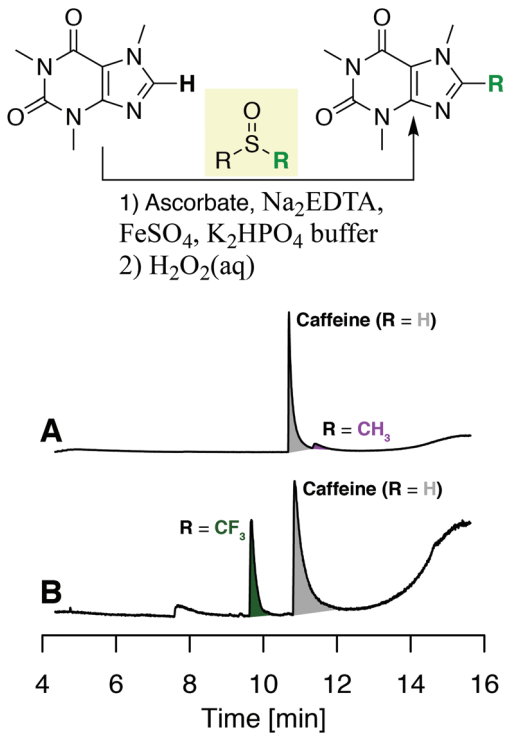

Fig. 4 GC-MS chromatograms of organic extracts of oxidative caffeine functionalization in aqueous, buffered media with Fenton's reagent and DMSO (A) or DMSO-F_6 (B).

site for radical addition and is reminiscent of purine nucleobases. Thus, the well-established oxidative activation of DMSO by the Fenton protocol for methylating adenine and guanidine should provide an ideal blue print.[29] To mixtures of caffeine, ascorbic acid, Na_2EDTA and $Fe(II)SO_4{\cdot}7H_2O$ in phosphate buffer we added at 0 °C a DMSO derivative followed by dropwise addition of H_2O_2. Products were extracted with ethyl acetate and analyzed by GC-MS (Fig. 4). Besides unreacted starting material (t_R = 11.0 min; 194*m*/*z*, grey) only the functionalized products occur, *i.e.* CF_3-caffeine (t_R = 9.8 min; 262*m*/*z*, green) or CH_3-caffeine (t_R = 11.6 min; 208*m*/*z*, magenta), as well as minor amounts of a decomposition product likely arising from oxidative imidazole cleavage (t_R = 11.6 min, 112*m*/*z*). The product CF_3-caffeine was quantified by ^{19}F NMR spectroscopy through addition of $PhCF_3$ as internal standard to the organic extract and furnished a value of approximately 16%.

Discussion

Rates constants for the reaction of DMSO-F_6 with $e_{aq}^{\bullet-}$ and $HO^{\bullet}$

Perfluorination has two distinct effects on the reactivity of DMSO. The inductive effect exerted by fluorine will decrease electron density around the sulfur center. Additionally, the C–F bond is easier to reduce than the C–H bond because of the very low lying σ_{CF}^* orbital,[30] and the resulting instability of perfluorinated materials towards strongly reducing conditions is well documented.[31] The reaction of the solvated electron with DMSO-F_6, $k_4 = (2-5) \times 10^9$ M^{-1} s^{-1}, is three orders of magnitude larger than with ordinary DMSO (calculated curve depicted in light grey in Fig. 1B). Conversely and as inferred, the oxidation of DMSO-F_6 with $HO^{\bullet}$, $k_7 = (0.6-2.5) \times 10^9$ M^{-1} s^{-1}, is an order of magnitude slower than that of DMSO.[32]

Reagents for production of $F_3C^{\bullet}$ radicals in pulse radiolysis

Experiments with Langlois' reagent and trifluoroacetate yielded unsatisfactory results for different reasons but serve as valuable references due to the reagents' commercial availability. The oxidation of trifluoroacetate with $HO^{\bullet}$ is simply too slow for fast production of $F_3C^{\bullet}$ needed in time-resolved mechanistic studies. We find $k_{11} = (6-7) \times 10^5$ M^{-1} s^{-1} in agreement with published data from flash photolysis experiments ($<10^6$ M^{-1} s^{-1}).[33] Langlois' reagent is kinetically ideal for our purposes, $k_{10} = 5 \times 10^9$ M^{-1} s^{-1}. The corresponding Zn-salt (Baran modification) is stable and available in high purity, however, Zn^{2+} has a rich complex chemistry that distinctly limits the use of this compound. In our case, the low solubility of $Zn[Fe(CN)_6]$ precluded certain measurements.[13] On the other hand, the sodium salt proved to be either unstable or not pure: experiments yielded distinctly differing kinetics traces for timescales >20 μs from day to day, which is not acceptable for future mechanistic investigations. In addition, earlier experiments with reductive activation of CF_3I showed several disadvantages associated with this gas, such as the necessity of signal deconvolution.[34]

DMSO-F_6 has the drawback of not being commercially available. Its rate of reaction with $HO^{\bullet}$ is lower than that of Langlois' reagent by half an order of magnitude. On the other hand, liquid handling is comparatively easy, and the reagent proved to be robust in daily use. This makes DMSO-F_6 the currently best, though not optimal, choice for time-resolved mechanistic studies. We therefore investigated the mechanism of the oxidative activation more closely, because in principle, fragmentation of the oxidized intermediate $[(CF_3)_2S(OH)O]^{\bullet-}$ may not only occur *via* reaction (14), but also *via* reactions (20) and (21), also producing a moderately oxidizing radical.

$$[(CF_3)_2S(OH)O]^{\bullet} \rightarrow [(CF_3)_2S(O)O]^{\bullet-} + H^+ \quad (20)$$

$$[(CF_3)_2S(O)O]^{\bullet-} \rightarrow CF_3SO_2^{\bullet} + F_3C^- \quad (21)$$

Kinetics experiments as well as product analysis were carried out to confirm the hypothesis of fragmentation *via* reaction (14). Product analysis, demonstrating trifluoromethylation of caffeine after oxidative activation of DMSO-F_6 by the Fenton reagent, indeed supports the notion of $F_3C^{\bullet}$ radical production, reaction (14), very clearly, albeit at low yield. In this regard, it is noteworthy that the addition of ascorbate proved critical to observing the functionalized product. However, ascorbate ("antioxidant") may reduce the $F_3C^{\bullet}$ radical, thereby preventing oxidative functionalization of caffeine.[35] Because perfluoroalkyl radicals exhibit a very low molar absorptivity, we decided to monitor kinetics with a reporter molecule, $ABTS^{2-}$. In the presence of oxygen, we observe a double-exponential be-

havior (Fig. 3), *i.e.* two sequential (pseudo)-first order reactions can be resolved. In aqueous environment $F_3C^{\bullet}$ and $Cl_3C^{\bullet}$ radicals have a similar electronegativity.[34,36] Similarly, $F_3COO^{\bullet}$ and $Cl_3COO^{\bullet}$ show comparable kinetic behavior.[37] While the former is a stronger oxidant, the overall reactivity of both molecules is dominated by the electron-withdrawing effect exerted by the halogen substitution pattern. With the ascorbate anion (trihalogen)methylperoxyl radicals have a reactivity $H_3COO^{\bullet} \ll Cl_3COO^{\bullet} \leq F_3COO^{\bullet}$ with corresponding relative rate constants of 1 : 100 : 100.[38] For the reaction with Trolox C the corresponding rate constants have a relative magnitude of 1 : 2400 : 4700. Oxygen will cause formation of $F_3COO^{\bullet}$ radicals, reaction (15), which we expect to exhibit a comparable reactivity as $Cl_3COO^{\bullet}$, $k_{16} = (1.2 - 1.9) \times 10^9\ M^{-1}\ s^{-1}$.[28] This is indeed the case: $k_{17} = (1 - 3) \times 10^9\ M^{-1}\ s^{-1}$. (Table 2) Is the remaining rate constant, with $k_{calc} = (0.5 - 3) \times 10^5\ s^{-1}$, to be attributed to reaction (14) or reaction (15)? Based solely on our data we cannot decide unequivocally. Nevertheless, reaction (15) is the more probable candidate for two reasons: (A) given $[O_2] \approx 200\ \mu M$,[39] we would calculate $k_{15} = (0.3 - 1.5) \times 10^9\ M^{-1}\ s^{-1}$, in agreement with the corresponding rate constants for the reactions of $H_3C^{\bullet}$ and $Cl_3C^{\bullet}$ with O_2 of $(3.0 - 4.7) \times 10^9\ M^{-1}\ s^{-1}$ and $3.3 \times 10^9\ M^{-1}\ s^{-1}$, respectively.[40] (B) Compared to a reported value of $k_{21} = 1.5 \times 10^7\ s^{-1}$ we consider a value of $k_{14} = (0.5 - 3) \times 10^5\ s^{-1}$ too low.[41]

$$[(CH_3)_2S(OH)O]^{\bullet} \rightarrow CH_3SO_2^{-} + H_3C^{\bullet} + H^{+} \qquad (21)$$

The [S → C] substitution from Langlois' reagent to trifluoroacetate underpins the importance of a nucleophilic central atom to achieve significant scavenging rates of the $HO^{\bullet}$ radical. A loss in reactivity of over three orders of magnitudes was observed and this innocuous substitution was likely accompanied by a fundamental change in mechanism. Furthermore, the comparison of trifluoroacetate with acetate is an illustrative example for the often-quoted increase in metabolic stability achieved by the [$CH_3 \rightarrow CF_3$] modification. In acetate, α-hydrogen abstraction predominates over oxidation ($k(H_3CCO_2^{-} + HO^{\bullet}) = (7.9 - 10) \times 10^7\ M^{-1}\ s^{-1}$).[22a,33,34]

Similarly, the [H → F] substitution in DMSO causes reactivity changes. As abovementioned, perfluorination of DMSO decreases the rate constant of its reaction with $HO^{\bullet}$ about half an order of magnitude. The CF_3-group is a relatively strongly σ-withdrawing moiety and may, in addition, allow for stabilizing $n \rightarrow \sigma_{CF}^*$ interactions.[30] The lone pair at sulfur in DMSO-F_6 may thus be rendered less electron-rich and presumably overall less available than in DMSO. A lower reactivity appears only reasonable. If oxidative activation occurs *via* addition of the $HO^{\bullet}$ radical to sulfur, reaction (7), an additional steric argument should be considered: the electron density at the fluorine atoms gives rise to shielding. This may hinder the trajectory of an incoming radical. The comparison of the behavior of DMSO-F_6 and of Langlois' reagent suggests that the replacement of a single CF_3 group in DMSO-F_6 fully reconstitutes the reactivity lost due to the perfluorination of native DMSO. However, whether this effect is mostly electronic in nature (*e.g.* anionic *vs.* neutral) or whether it also features a (pronounced) steric component cannot be deduced from the data at hand.

Conclusions

In analogy to the oxidative activation of DMSO with $HO^{\bullet}$ providing $H_3C^{\bullet}$, we explored the feasibility of using DMSO-F_6 as a precursor to $F_3C^{\bullet}$. Pulse-radiolysis studies in conjunction to laboratory experiments corroborated that DMSO-F_6 undergoes a rapid reaction with $HO^{\bullet}$ with $k_7 = (0.6 - 2.5) \times 10^9\ M^{-1}\ s^{-1}$, followed by a fragmentation reaction to furnish $F_3C^{\bullet}$. In comparison to other commercially available precursors (Langlois' reagent, trifluoroacetate), DMSO-F_6 proved stable, easier to handle and overall more robust and therefore, is well suited for time-resolved kinetics studies of $F_3C^{\bullet}$. The major caveat is the requirement for its laboratory synthesis and hitherto time-consuming purification.

Conflicts of interest

There are no conflicts to declare.

Acknowledgements

This work was generously supported by the Swiss National Science Foundation (N. S.; P3P3P2_167744), the National Science and Engineering Research Council of Canada (B. J. J.) and ETH Zürich (Prof. D. Günther, Prof. A. Togni).

Notes and references

1 (*a*) J. O. Kang, K. S. Gallagher and G. Cohen, *Arch. Biochem. Biophys.*, 1993, **306**, 178–182; (*b*) K. Kawai, Y.-S. Li, M.-F. Song and H. Kasai, *Bioorg. Med. Chem. Lett.*, 2010, **20**, 260–265.
2 H. Schönherr and T. Cernak, *Angew. Chem., Int. Ed.*, 2013, **52**, 12256–12262.
3 J. Gui, Q. Zhou, C.-M. Pan, Y. Yabi, A. C. Burns, M. R. Collins, M. A. Ornelas, Y. Ishihara and P. S. Baran, *J. Am. Chem. Soc.*, 2014, **136**, 4853–4856.
4 R. Caporaso, S. Manna, S. Zinken, A. R. Kochnev, E. R. Lukyanenko, A. V. Kurkin and A. P. Antonchick, *Chem. Commun.*, 2016, **52**, 12486–12489.
5 C. Hansch, A. Leo and D. Hoekmann, *QSAR: Volume 2: Hydrophobic, Electronic, and Steric Constants*, American Chemical Society, Washington DC, 1995.
6 K. Müller, C. Faeh and F. Diederich, *Science*, 2017, **317**, 1881–1886.
7 A. Studer, *Angew. Chem., Int. Ed.*, 2012, **51**, 8950–8958.
8 (*a*) J. W. Beatty, J. J. Douglas, K. P. Cole and C. R. J. Stephenson, *Nat. Commun.*, 2015, **6**, 7919; (*b*) N. Kamigata, T. Fukushima and M. Yoshida, *Chem.*

Lett., 1990, **19**, 649–650; (*c*) Y. Ouyang, X.-H. Xu and F.-L. Qing, *Angew. Chem., Int. Ed.*, 2018, **57**, 6926–6929.

9 Y. Fujiwara, J. A. Dixon, F. O'Hara, E. D. Funder, D. D. Dixon, R. A. Rodriguez, R. D. Baxter, B. Herlé, N. Sach, M. R. Collins, Y. Ishihara and P. S. Baran, *Nature*, 2012, **492**, 95–99.

10 K. Matcha and A. P. Antonchick, *Angew. Chem., Int. Ed.*, 2014, **53**, 11960–11964.

11 A. Henglein, W. Schnabel and J. Wendenburg, *Einführung in die Strahlenchemie*, Verlag Chemie GmbH, Weinheim, 1969.

12 (*a*) G. Bullock and R. Cooper, *Trans. Faraday Soc.*, 1970, **66**, 2055–2064; (*b*) N. Santschi and T. Nauser, *J. Fluorine Chem.*, 2017, **203**, 218–222.

13 G. Jander and E. Blasius, *Lehrbuch der analytischen und präparativen anorganischen Chemie*, S. Hirzel Verlag, Stuttgart, 1969.

14 (*a*) From dimethyl sulfite: D. T. Sauer and J. M. Shreeve, *J. Fluorine Chem.*, 1971/72, **1**, 1–11; (*b*) R. Singh, G. Cao, R. Kirchmeier and J. Shreeve, *J. Org. Chem.*, 1999, **64**, 2873–2876.

15 A similar protocol from thionyl fluoride, see: N. Patel and R. Kirchmeier, *Inorg. Chem.*, 1992, **31**, 2537–2540.

16 W. M. Hanyes, *CRC Handbook of Chemistry and Physics*, CRC Press/Taylor&Francis, Boca Raton, Florida, 97th edn, 2016.

17 H. Shiraishi, G. V. Buxton and N. D. Wood, *Int. J. Radiat. Appl. Instrum., Part C. Radiat. Phys. Chem.*, 1989, **33**, 519–522.

18 (*a*) M. A. J. Rodgers, D. C. Foyt and Z. A. Zimek, *Radiat. Res.*, 1978, **75**, 296–304; (*b*) A. Horvath, O. Horvath and K. L. Stevenson, *J. Photochem. Photobiol., A*, 1992, **68**, 155–163.

19 (*a*) A. M. Koulkes-Pujo, B. D. Michael and E. J. Hart, *Int. J. Radiat. Phys. Chem.*, 1971, **3**, 333–344; (*b*) D. Razem and W. H. Hamill, *J. Phys. Chem.*, 1977, **81**, 1625–1631.

20 A. J. Elliot, *Radiat. Phys. Chem.*, 1989, **34**, 753–758.

21 (*a*) W. N. Perera and G. Hefter, *Inorg. Chem.*, 2003, **42**, 5917–5923; (*b*) J. J. Alexander and H. B. Gray, *J. Am. Chem. Soc.*, 1968, **90**, 4260–4271.

22 (*a*) R. L. Willson, C. L. Greenstock, G. E. Adams, R. Wageman and L. M. Dorfman, *Int. J. Radiat. Phys. Chem.*, 1971, **3**, 211–220; (*b*) W. L. Waltz, S. S. Akhtar and R. L. Eager, *Can. J. Chem.*, 1973, **51**, 2525–2529.

23 (*a*) C. L. Crawford, M. R. Gholami, S. L. Roberts and R. J. Hanrahan, *Radiat. Phys. Chem.*, 1992, **40**, 205–212; (*b*) N. Selvarajan and N. V. Raghavan, *J. Chem. Soc., Chem. Commun.*, 1980, 336–337.

24 B. H. Milosavljevic and J. A. LaVerne, *J. Phys. Chem. A*, 2005, **109**, 165–168.

25 R. H. Schuler, A. L. Hartzell and B. Behar, *J. Phys. Chem.*, 1981, **85**, 192–199.

26 R. H. Schuler, L. K. Patterson and E. Janata, *J. Phys. Chem.*, 1980, **84**, 2088–2089.

27 U. K. Kläning and T. Wolff, *Ber. Bunsenges. Phys. Chem.*, 1985, **89**, 243–245.

28 (*a*) B. S. Wolfenden and R. L. Willson, *J. Chem. Soc., Perkin Trans. 2*, 1982, 805–812; (*b*) J. E. Packer and R. L. Willson, *J. Chem. Soc., Perkin. Trans 2*, 1984, 1415–1419.

29 (*a*) J. O. Kang, K. S. Gallagher and G. Cohen, *Arch. Biochem. Biophys.*, 1993, **306**, 178–183; (*b*) K. Kawai, Y.-S. Li, M.-F. Song and H. Kasai, *Bioorg. Med. Chem. Lett.*, 2010, **20**, 260–265.

30 D. O'Hagan, *Chem. Soc. Rev.*, 2008, **37**, 308–319.

31 K. Brace, C. Combellas, M. Delamar, A. Fritsch, E. Kanoufi, M. E. R. Shanahan and A. Thiébault, *Chem. Commun.*, 1996, 403–404.

32 D. Veltwisch, E. Janata and K. D. Asmus, *J. Chem. Soc., Perkin Trans. 2*, 1980, 146–153.

33 P. Maruthamuthu, S. Padmaja and R. E. Huie, *Int. J. Chem. Kinet.*, 1995, **27**, 605–612.

34 N. Santschi and T. Nauser, *ChemPhysChem*, 2017, **18**, 2973–2976.

35 T. Nauser and J. Gebicki, *Arch. Biochem. Biophys.*, 2017, **633**, 118–123.

36 F. De Vleeschouwer, V. Van Speybroeck, M. Waroquier, P. Geerlings and F. De Proft, *Org. Lett.*, 2007, **9**, 2721–2724.

37 R. E. Huie, D. Brault and P. Neta, *Chem.-Biol. Interact.*, 1987, **62**, 227–235.

38 (*a*) X. Shen, J. Lind, T. E. Eriksen and G. Merenyi, *J. Phys. Chem.*, 1989, **93**, 553–557; (*b*) P. Neta, R. E. Huie, P. Maruthamuthu and S. Steenken, *J. Phys. Chem.*, 1989, **93**, 7654–7659.

39 R. Sander, *Atmos. Chem. Phys.*, 2015, **15**, 4399–4981.

40 (*a*) A. Sauer, H. Cohen and D. Meyerstein, *Inorg. Chem.*, 1989, **28**, 2511–2512; (*b*) J. K. Thomas, *J. Phys. Chem.*, 1967, **71**, 1919–1925; (*c*) J. Moenig, D. Bahnemann and K. D. Asmus, *Chem.-Biol. Interact.*, 1983, **47**, 15–27.

41 R. Herscu-Kluska, A. Masarwa, M. Saphier, H. Cohen and D. Meyerstein, *Chem. – Eur. J.*, 2008, **14**, 5880–5889.